Formation of In$_2$O$_3$ films by magnetron sputtering on Al$_2$O$_3$ (012) substrates

© *A.A. Tikhii*[1], *Yu.M. Nikolaenko*[2], *E.A. Svyrydova*[2,3], *I.V. Zhikharev*[2]

[1] Lugansk State Pedagogical University,
91011 Lugansk, Luhansk People's Republic
[2] Donetsk Institute of Physics and Technology named after A.A. Galkin,
83114 Donetsk, Donetsk People's Republic
[3] Donbas National Academy of Civil Engineering and Architecture,
286123 Makeevka, Donetsk People's Republic

e-mail: ea0000ffff@mail.ru

The results of studies of the microstructure and optical characteristics of In$_2$O$_3$ films deposited by the dc-magnetron sputtering of a polycrystalline target onto single-crystal sapphire substrates are summarized. The technological regimes of films preparation differed in the deposition time, substrate temperature, and the presence of additional heat treatment of film structures in air. It has been established that the optical refractive index of films deposited on a „cold" substrate increases in the direction from the substrate to the external interface. Heat treatment of the films eliminates the inhomogeneity of the refractive index and leads to a decrease in the band gap. The observed optical properties are explained by the thickness inhomogeneous microstructure of the films, which is formed during sputtering of a target with a relatively low mechanical strength.

Keywords: In$_2$O$_3$ films, magnetron sputtering, Al$_2$O$_3$ substrates, refraction index, bandgap width.

Introduction

In$_2$O$_3$ films combine the properties of high optical transparency ($> 80\%$) and high electrical conductivity, which, in addition, is very sensitive to the composition of the surrounding atmosphere of the In$_2$O$_3$ film. Because of this, they continue to find new applications. Since the doping of In$_2$O$_3$ with various impurities allows for the selectivity of its electrical conductivity sensitivity to various gases [1–4], films based on In$_2$O$_3$ are promising materials for creating gas sensors. To ensure high sensitivity of the latter, it is important to have a developed surface, on which reversible binding of the analyte takes place. This provides a rough surface of In$_2$O$_3$ films, which is naturally formed in the process of growth. The polycrystalline structure of the films and the presence of mechanical stresses in them increase the diffusion coefficients [5], which also increases the sensitivity of sensors based on them.

As a rule, quartz or quartz-passivated glass substrates are used to produce polycrystalline indium oxide films. However, the use of sapphire substrates can be justified by their better thermal and chemical stability. This is especially true in the context of chemical sensor development. Depending on the chosen crystal-lattice orientation of the sapphire substrate cut plane and the sputtering method, both polycrystalline and epitaxial films can be obtained. And while the number of works devoted to epitaxial films on sapphire substrates is quite large [6–10], the amount of studies devoted to polycrystalline films is small. It

should be noted that depending on the method and modes of production, the surface structure of the films may be different [11].

Magnetron sputtering used to produce indium oxide films is scalable, provides good performance [12,13], reproducibility of film parameters, allows to obtain them not only at high, but also at low substrate temperatures. The latter is important when working with polymeric materials. The surface of the films produced by this method has greater roughness compared to the films produced by other methods, such as pulsed laser sputtering [14].

The application of optical non-destructive research methods (ellipsometry and optical transmission) allows a non-contact study of the properties of nanoscale thin-film coatings. Ellipsometry is a highly sensitive polarization-optical method for studying surfaces and interfaces of different media. It allows us to determine the optical properties as well as the thicknesses of individual, including rough layers (if the characteristic dimensions of the roughness are much smaller than the wavelength of the probing radiation). Knowing the distribution of the refraction index over the thickness of the film as applied to a given material allows us to judge the distribution of porosity with thickness. In the case of sufficiently thick coatings, the thickness and optical properties of the layers can also be determined from the results of spectral measurements of optical transmittance. These methods complement each other, because the influence of material parameters on the results of ellipsometric measurements decreases with

Table 1. Parameters of In_2O_2 films obtained at different substrate temperatures (sputtering time — 1 h)

Temperature of the substrate	20°C	300°C	600°C
Parameters of film In_2O_3	$n = 1.9 - 2$ $d = 550\,nm$	$n = 2$ $d = 450\,nm$	$n = 2.1$ $d = 440\,nm$
Parameters of the rough layer	$n = 2-1.8$ $d = 80\,nm$	$n = 2-1.53$ $d = 75\,nm$	$n = 2.1-1.65$ $d = 20\,nm$

Table 2. Direct and „indirect" transitions in In_2O_3 films

Temperature of the substrate, °C	Before annealing		After annealing	
	E_g^{Γ}, eV	E_g^{indir}, eV	E_g^{Γ}, eV	E_g^{indir}, eV
20	4.07	2.94	3.71	2.69
600	3.72	2.72	3.71	2.67

Table 3. Parameters of the model layers of the films under study at different sputtering times

Time of sputtering, min	d_1, nm	d_2, nm	d_3, nm	n^3
15	20	7	26	3
35	11	21	25	3
60	6	30	25	3
120	7	180	22	2.9
180	6	355	25	3

increasing the distance from it to the surface, while there is no such dependence for the value of optical transmittance. The combination of these methods allowed us to construct models of the structure and optical properties of the films studied, which are also consistent with the results of X-ray diffraction analysis.

In the present work, we have collected the results of our earlier studies on the structure and optical properties of In_2O_3 films obtained on Al_2O_3 (012) substrates in different dc-magnetron sputtering modes [15–25].

Experiment

Sputtering was carried out in an argon-oxygen atmosphere for $15-180$ min at different substrate temperatures. The operating current was 50 mA and the voltage was 300 V. After the measurements, the obtained films were also annealed in air for 1 h at 600°C and then examined again.

Ellipsometric measurements were performed using a multi-angle null ellipsometer at the helium–neon laser wavelength (632.8 nm). Optical transmission measurements were made on a Shimadzu UV-2450 spectrophotometer.

The composition of targets and obtained films was monitored using an X-ray diffractometer DRON-3.

Results and discussion

X-ray diffraction analysis showed that the studied films are polycrystalline and show a reflex corresponding to the plane (222) of the cubic modification of In_2O_3 (space group $Ia\bar{3}$) [16–18].

Analysis of a series of films obtained at different substrate temperatures indicates that as the substrate temperature decreases, not only does the thickness d of the obtained films increase, but also the degree of material heterogeneity [19–22] — the refraction index n of films deposited on 20°C substrates increases linearly from 1.9 to 2 in the substrate to rough layer direction (Table 1). This can occur due to an increase in the surface temperature of the growing film during the spraying process.

Annealing leads to the unification of the properties of the films studied, improvement of homogeneity of refraction index distribution over thickness, reduction of film thickness and surface roughness — material compaction takes place.
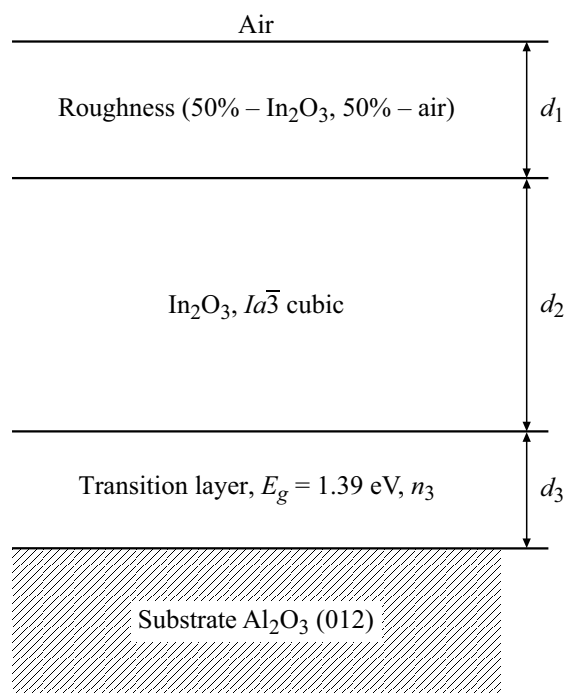
(For example, the thicknesses of the films shown in Table 1 approach 400 nm, the refraction indices — to 2, and the thickness of the disturbed layer — to 21 nm.)

Also, substrate temperature and annealing affect the position of the fundamental absorption edge of the films studied [16,19,20,23]. The apparent bandgap width for direct transitions E_g^{Γ} is smaller the higher the substrate temperature during film deposition (Table 2). Annealing also leads to the unification of the bandgap width. Such results are quite natural — E_g^{Γ} in In_2O_3 differs significantly from the real one due to the features of the lattice symmetry and the Burstein−Moss [26] shift. The latter depends significantly on crystal structure defects, the number of which is lower in films deposited on substrates with higher temperatures. Annealing in air eliminates oxygen vacancies, which reduces the concentration of charge carriers and therefore the value of E_g^{Γ} [27,28]. The bandgap width for „indirect" (symmetry forbidden) transitions E_g^{indir} varies less due to electron-phonon interactions.

For some of the films studied, we also observed the dependence of their structure on the sputtering time [18,24,25]. Thus, according to the X-ray diffraction measurements, the position of the reflex corresponding to the plane (222) shifts from 30.3° to 30.6° as the sputtering time decreases. The half-width of the reflex decreases in this case.

The results of measurements of the optical transmittance of such films show its anomalous decrease with decreasing wavelength. We described the optical properties of such films using a three-layer model (figure).

The first layer of this model describes the rough surface of the film. It is modeled as a homogeneous layer with optical properties calculated based on the dielectric permittivity of the cubic modification In_2O_3 and a fill factor of 0.5 according to the Clausius−Mossotti equation. The optical properties of the second layer correspond to the cubic

Air

Roughness (50% – In$_2$O$_3$, 50% – air) d_1

In$_2$O$_3$, $Ia\overline{3}$ cubic d_2

Transition layer, E_g = 1.39 eV, n_3 d_3

Substrate Al$_2$O$_3$ (012)

Model of the investigated films.

modification of In$_2$O$_3$ according to [29]. The third layer (with high extinction coefficient) is located between the film and the substrate. The best correspondence of the spectral dependence of the extinction coefficient of this layer is the law of fundamental absorption in a semiconductor with a bandgap width $E_g = 1.39$ eV for direct transitions. Because of the high extinction coefficient it is difficult to judge its other properties, but ellipsometric measurements suggest that the refraction index of this layer is close to 3, which agrees with the refraction index estimates for a semiconductor with a bandgap of 1.39 eV made according to [30].

As can be seen from Table 3, for films with spraying time from 15 to 60 min, the thickness of the surface layer decreases, and the thickness of the middle layer increases with increasing spraying time, while the total thickness of the first two layers remains practically unchanged.

This suggests that films with longer sputtering times contain smaller crystallites on average. In other words, we can assume, that at the beginning of sputtering, large particles of material are formed on the substrate surface, and then, in the sputtering, the size of emerging crystallites decreases, and they fill the gaps between the larger particles. Later (60−180 min), the surface layer thickness is preserved, and the total thickness of the film increases — the film formation process reaches a stationary mode.

The formation of a transition layer at the border with the substrate is probably due to the bandgap blurring due to the large number of defects in the crystal structure, as well as to the formation of impurity levels inside the bandgap. The thickness of this layer is almost independent of the

sputtering time and, therefore, its appearance is entirely due to the influence of the substrate surface.

Conclusions

Films obtained at low temperatures, in addition to surface roughness, have heterogeneity in the surface-substrate direction, which can be eliminated by annealing in the air. The decrease in the energy of interband transitions when eliminating defects in the crystal structure of the films can be explained by the Burstein−Moss shift. The obtained values of the bandgap width are in agreement with the results of [26–28].

To describe the optical properties of some In$_2$O$_3$ films, it may be necessary to introduce an additional layer at the interface with the substrate. The refraction index value of this layer from ellipsometric measurements is close to three, which agrees well with the estimated bandgap width of 1.39 eV based on optical transmission measurements.

The results of ellipsometric measurements and X-ray diffraction analysis indicate that large material particles form on the substrate surface at the beginning of sputtering. Then the gaps between them are filled with finer crystallites, after which the film formation process reaches a stationary mode.

References

[1] A.A. Khalefa, J.M. Marei, H.A. Radwan, J.M. Rzaij. Digest J. Nanomaterials and Biostructures, **16** (1), 197 (2021).

[2] A.A. Yousif, M.H. Hasan. J. Biosens. Bioelectron., **6** (4), 1000192 (2015). DOI: 10.4172/2155-6210.1000192

[3] J. Liu, W. Guo, F. Qu, C. Feng, C. Li, L. Zhu, J. Zhou, S. Ruan, W. Chen. Ceramics International, **40**, 6685 (2014). DOI: /10.1016/j.ceramint.2013.11.129

[4] D. Manno, M.D. Giulio, T. Siciliano, E. Filippo, A. Serra. J. Phys. D: Appl. Phys., **34**, 2097 (2001). DOI: 10.1088/0022-3727/34/14/303

[5] Yu.M. Nikolaenko, A.N. Artemov, Yu.B. Medvedev, N.B. Efros, I.V. Zhikharev, I.Yu. Reshidova, A.A. Tikhii, S.V. Kara-Murza. J. Phys. D: Appl. Phys., **49**, 375302 (2016). DOI: 10.1088/0022-3727/49/37/375302

[6] X. Du, J. Yu, X. Xiu, Q. Sun, W. Tang, B. Man. Vacuum, **167**, 1 (2019). DOI: 10.1016/j.vacuum.2019.05.035

[7] S.K. Yadav, S. Das, N. Prasad, B.K. Barick, S. Arora, D.S. Sutar, S. Dhar. J. Vacuum Science & Technology A, **38**, 033414 (2020). DOI: 0.1116/6.0000038

[8] M. Nistor, W. Seiler, C. Hebert, E. Matei, J. Perrière. Appl. Surface Science, **307**, 455 (2014). DOI: 10.1016/j.apsusc.2014.04.056

[9] W. Seiler, M. Nistor, C. Hebert, J. Perrière. Solar Energy Materials and Solar Cells, **116**, 34 (2013). DOI: 10.1016/j.solmat.2013.04.002

[10] S. Kaneko, H. Torii, M. Soga, K. Akiyama, M. Iwaya, M. Yoshimoto, T. Amazawa. Jpn. J. Appl. Phys., **51** (1S), 01AC02 (2012).

[11] M.Z. Jarzebski. Phys. Stat. Sol. (a), **71**, 13 (1982). DOI: 10.1002/pssa.2210710102

[12] M. Higuchi, S. Uekusa, R. Nakano, K. Yokogawa. J. Appl. Phys., **74** (11), 6710 (1993). DOI: 10.1063/1.355093

[13] Y. Shigesato, S. Takaki, T. Haranoh. J. Appl. Phys., **71** (7), 3356 (1992). DOI: 10.1063/1.350931

[14] H. Kim, C.M. Gilmore, A. Pique, J.S. Horwitz, H. Mattoussi, H. Murata, Z.H. Kafafi, D.B. Chrisey. J. Appl. Phys., **86** (11), 6451 (1999). DOI: 10.1063/1.371708

[15] Yu.M. Nikolaenko, A.B. Mukhin, V.A. Chaika, V.V. Burkhovetskii. Technical Physics, **55** (8), 1189 (2010).

[16] A.A. Tikhii, Yu.M. Nikolaenko, A.S. Kornievets, I.V. Zhikharev. In: *The 21st International Conference on Surface Modification of Materials by Ion Beams*, ed. by M. Yuzhakov, O. Lapteva, M. Slobodyan, V. Tarbokov, G. Remnev (Mozart, Tomsk, Russia, 2019), p. 4.

[17] A.A. Tikhii, Yu.M. Nikolaenko, Yu.I. Zhikhareva, I.V. Zhikharev. In: *7th International Congress on Energy Fluxes and Radiation Effects (EFRE-2020 online): Abstracts* (Publishing House of IAO SB RAS, Tomsk, 2020), p. 601.

[18] A.A. Tikhii, Yu.M. Nikolaenko, Yu.I. Zhikhareva, I.V. Zhikharev. Opt. Spectrosc., **128** (10), 1667 (2020). DOI: 10.1134/S0030400X20100252.

[19] A.A. Tikhii, Yu.M. Nikolaenko, Yu.I. Zhikhareva, A.S. Kornievets, I.V. Zhikharev. Semiconductors, **52**, 320 (2018). DOI: 10.1134/S1063782618030223.

[20] V.A. Gritskikh, I.V. Zhikharev, S.V. Kara-Murza, N.V. Korchikova, T.V. Krasnyakova, Y.M. Nikolaenko, A.A. Tikhii, A.V. Pavlenko, Y.I. Yurasov. In: *Advanced Materials Techniques, Physics, Mechanics and Applications*, ed. by Ivan A. Parinov, Shun-Hsyung Chang, Muaffaq A. Jani. Springer Proceedings in Physics (Springer International Publishing AG., 2017), v. 193, p. 55. DOI: 10.1007/978-3-319-56062-5

[21] A.A. Tikhii, V.A. Gritskikh, S.V. Kara-Murza, N.V. Korchikova, Yu.M. Nikolaenko, Yu.I. Zhikhareva, I.V. Zhikharev. In: *European Materials Research Society Spring Meeting 2016 (E-MRS 2016)* (France, Lille, 2016), L.P. 32 — Access mode: https://www.european-mrs.com/2016-spring-symposium-l-european-materials-research-society

[22] A.A. Tikhii, Yu.M. Nikolayenko, M.Yu. Badekin, V.N. Sayapin, N.P. Ivanitsyn, I.V. Zhikharev. Vestnik DonNU. Ser. A: Natural Sciences, **3**, 112 (2017).

[23] A.A. Tikhii, V.A. Gritskikh, S.V. Kara-Murza, N.V. Korchikova, Y.M. Nikolayenko, I.V. Zhikharev. In the collection: International Scientific-Practical Conference „Open Physics Readings". Theses of Reports, ed. by T.V. Krasnyakova, E.E. Gorbenko, L.A. Reznichenko, I.A. Verbenko („Alma Mater", Luhansk, 2016), p. 37.

[24] A.A. Tikhii, Yu.I. Zhikhareva, I.V. Zhikharev. In the collection: *Physics.SPb: Abstracts of the International Conference 18−22 October 2021* (Polytech-press, SPb., 2021), p. 252.

[25] A.A. Tikhii, K.A. Svyrydova, Yu.I. Zhikhareva, I.V. Zhikharev. J. Appl. Spectrosc., **88** (5), 975 (2021). DOI: 10.1103/PhysRevLett.29.274.

[26] A. Walsh, J.L.F. Da Silva, Su-Huai Wei, C. Korber, A. Klein, L.F.J. Piper, A. De Masi, K.E. Smith, G. Panaccione, P. Torelli, D.J. Payne, A. Bourlange, R.G. Egdell. Phys. Rev. Lett., **100**, 167402 (2008). DOI: 10.1103/PhysRevLett.100.167402

[27] Y. Furubayashi, M. Maehara, T. Yamamoto. ACS Applied Electronic Materials, **1** (8), 1545 (2019). DOI: 10.1021/acsaelm.9b00317

[28] L. Gupta, A. Mansingh, P.K. Srivastava. Thin Solid Films, **176**, 33 (1989). DOI: 10.1016/0040-6090(89)90361-1

[29] A. Schleife, M.D. Neumann, N. Esser, Z. Galazka, A. Gottwald, J. Nixdorf, R. Goldhahn, M. Feneberg. New J. Phys., **20**, 053016 (2018). DOI: 10.1088/1367-2630/aabeb0

[30] N.M. Ravindra, P. Ganapathy, J. Choi. Infrared Physics & Technology, **50**, 21 (2007). DOI: 10.1016/j.infrared.2006.04.001